

# Renormalized one-Loop Corrections in Power Spectrum in USR Inflation

Haidar Sheikahmadi<sup>a,\*</sup> and Amin Nassiri-Rad<sup>b,a†</sup>

<sup>a</sup> School of Astronomy, Institute for Research in Fundamental Sciences (IPM), P. O. Box 19395-5531, Tehran, Iran and

<sup>b</sup> Department of physics, K.N Toosi University of Technology, P.O. Box 15875-4416, Tehran, Iran

The nature of one-loop corrections on long CMB scale modes in models of single field inflation incorporating an intermediate USR phase is under debate. In this work, we investigate the regularization and renormalization of the one-loop corrections of curvature perturbation power spectrum. Employing the UV-IR regularizations and performing the in-in analysis, we calculate the regularized one-loop corrections, including tadpole, in the power spectrum associated with cubic and quartic Hamiltonians. We show that the fully regularized and renormalized fractional loop correction in the power spectrum is controlled by the peak of the power spectrum at the end of USR phase, scaling like  $e^{6\Delta\mathcal{N}}$  in which  $\Delta\mathcal{N}$  is the duration of the USR phase. This confirms the original conclusion that the loop corrections can get out of perturbative control if the transition from the intermediate USR phase to the final SR phase is instantaneous and sharp.

*Introduction.-* There is an ongoing debate on the nature of one-loop corrections in models of single field inflation incorporating an intermediate ultra slow-roll (USR) phase [1–10]. These setups have been proposed as a mechanism to generate primordial black holes (PBHs) as the seed of dark matter in cosmos [11–25]. In the simplest toy model, inflation contains three stages, an initial slow-roll (SRI) phase, followed by an intermediate USR phase and then a final SR phase (SRII). The duration of USR phase is short, engineered to enhance the curvature perturbation power spectrum by about seven orders of magnitude compared to the observed CMB scales, to generate PBHs of desired mass scales as the seeds of dark matter. Originally, it was claimed in [1] that the short modes which leave the horizon during the USR phase can affect the long CMB modes at one-loop level, inducing a fractional correction in power spectrum scaling like  $e^{6\Delta\mathcal{N}}\mathcal{P}_{\text{CMB}}$  in which  $\Delta\mathcal{N}$  is the duration of the USR phase and  $\mathcal{P}_{\text{CMB}} \sim 2 \times 10^{-9}$  is the amplitude of power spectrum on CMB scales. For PBHs formation, one typically requires  $\Delta\mathcal{N} \sim 2 - 3$  e-folds. It was argued that this loop correction can get out of perturbative control so the proposed setup can not be trusted for PBHs formation. This conclusion was criticized and re-examined in numerous follow up works. Specifically, the conclusion of [1] was confirmed in [3, 4], who employing the effective field theory (EFT) formalism of inflation, has calculated the cubic and quartic Hamiltonians necessary to calculate the full one-loop calculation. However, other works claimed that the dangerous loop corrections may be slow-roll suppressed, specially if the transition to the final SR phase is mild, [5, 6, 26, 27] so the loop corrections are still under perturbative control. On the other hand, a third category claimed that the loop corrections are volume suppressed (i.e. exponentially close to zero) and are totally negligible [28–33]. One open question

in these ongoing debates is the effects of regularization and renormalization and whether or not the conclusion of [1] survives after regularization and renormalization are taken into account. In this work we would like to address this issue in details. In quantum field theory (QFT), dealing with infrared (IR) and ultraviolet (UV) divergences is a fundamental challenge. The proper treatment of these divergences is crucial for obtaining physically meaningful results [34–37]. In this work we use the cutoff regularization scheme to treat both the IR and UV divergences. Employing the in-in

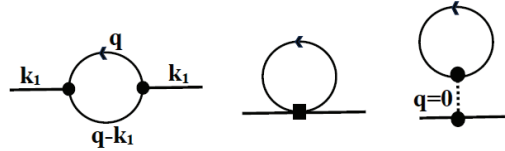


FIG. 1: One-loop diagrams include contributions from cubic and quartic interaction vertices, as well as the tadpole diagram. Black-filled circles and squares represent cubic (order 3) and quartic (order 4) vertices, respectively. In the cubic diagram,  $k_1$  denotes the external momentum, while  $q$  represents the internal momentum. The quartic diagram follows a similar structure, and in the tadpole diagram,  $q = 0$  corresponds to zero momentum.

formalism [38–40] to study loop corrections, we require the interaction Hamiltonian up to fourth order. Then adopting a UV-IR regularization scheme [41, 42], our calculations involve both UV and IR divergences, that accounts for the complete range of momentum integrals, say from 0 to  $\infty$  [50]. Specifically, we include both lower and upper cutoffs for momentum integrals, introducing regulators such as  $m \rightarrow 0$  (IR cutoff) and  $M \rightarrow \infty$  (UV cutoff). The results of these integrals are then expanded as series in terms of the cutoffs, allowing us to systematically examine their contributions. As one can realize from cubic diagram in figure 1, to take the momenta integrals, one should take care of contribution of  $q$  modes in internal leg. Another critical issue is the

\*Electronic address: [h.sh.ahmadi@gmail.com](mailto:h.sh.ahmadi@gmail.com)

†Electronic address: [amin.nassiriraad@kntu.ac.ir](mailto:amin.nassiriraad@kntu.ac.ir)

renormalization of time integrals, which can also exhibit divergences. While well-established methods, such as the  $i\epsilon$  prescription [43], are commonly used to handle these divergences, we also employ the Cauchy principal value (P.V.) method. This approach is particularly effective for nested integrals that arise in cubic loop corrections, providing a robust framework to manage time divergences in these cases. To eliminate the UV divergences, we commonly assume the existence of counterterms that can effectively cancel these divergences.

Motivated by these considerations, we revisit loop corrections in the context of the three-phase SR – USR – SR inflationary model. In our analysis, we incorporate both the quartic Hamiltonian,  $\mathbf{H}_4$ , corresponding to fourth-order vertices, and the cubic

Hamiltonian,  $\mathbf{H}_3$ , corresponding to third-order vertices, including tadpole contributions. Both momentum and time integrals are subjected to rigorous regularization and renormalization to ensure the consistency of our calculations. By accounting for the full range of momenta and employing advanced regularization schemes, our study provides new insights into the behavior of loop corrections in multi-phase inflationary models. More specifically, we demonstrate that the regularized loop correction scale like the peak of power spectrum at the end of USR, i.e. scaling like  $e^{6\Delta\mathcal{N}}\mathcal{P}_{\text{CMB}}$ , confirming the conclusion of [1] and [3, 46].

*The Setup*—To start with, we consider the contributions of cubic and quartic Hamiltonians  $\mathbf{H}_3$  and  $\mathbf{H}_4$ ,

$$\mathbf{H}_3 = -M_P^2 H^3 \eta \epsilon a^2 \int d^3x [\pi \pi'^2 - \pi (\partial\pi)^2] = -M_P^2 H^3 \eta \epsilon a^2 \int d^3x \left[ \pi \pi'^2 + \frac{1}{2} \pi^2 \partial^2 \pi \right], \quad (1)$$

$$\mathbf{H}_4 = \frac{M_P^2}{2} \int d^3x \left[ (H^4 \eta^2 \epsilon a^2 - \eta' H^3 \epsilon a) \pi^2 \pi'^2 + (H^4 \eta^2 \epsilon a^2 + \eta' H^3 \epsilon a) \pi^2 (\partial_i \pi)^2 \right], \quad (2)$$

Here  $M_P$  is the reduced Planck mass,  $a(\tau)$  is the FLRW scale factor,  $H$  is the Hubble rate during inflation while  $\epsilon$  and  $\eta$  are the first and the second slow-roll parameters.

The above cubic and quartic Hamiltonians for the Goldstone boson  $\pi$  was obtained in [3] employing the EFT of inflation [44, 45] in the decoupling limit where the gravitational backreactions are negligible. There is a non-linear relation between the curvature perturbation  $\mathcal{R}$  and the Goldstone boson  $\pi$  which should be taken into account. However, as discussed in [3], at the end of inflation when the system reaches the attractor phase, the non-linear corrections between  $\pi$  and  $\mathcal{R}$  become negligible and one can simply write  $\mathcal{R} = -H\pi + \mathcal{O}(\pi^2)$ .

The slow-roll parameters in each stage of the three phases take different values. In the SRI phase  $\epsilon \approx \eta \ll 1$ . In the USR phase  $\epsilon = \epsilon_i (\tau/\tau_i)^6$  and  $\eta = -6$ , in which the subscript  $i$  refers the start of USR phase. The duration of USR phase is defined as  $\Delta\mathcal{N} = \mathcal{N}(\tau_e) - \mathcal{N}(\tau_i)$  in which  $\tau_e$  represents the time of end of USR phase. One can show that during the USR phase  $\epsilon$  falls off exponentially, that is  $\epsilon_e = \epsilon_i \exp(-6\Delta\mathcal{N})$ . Finally for the SRII phase, slow-roll parameter takes the form  $\epsilon(\tau) = \epsilon_e \left( \frac{h}{6} - (1 + \frac{h}{6}) \left( \frac{\tau}{\tau_e} \right)^3 \right)^2$ , with  $h \equiv -6\sqrt{\epsilon_V/\epsilon_e}$  in which  $\epsilon_V$  is the final value of  $\epsilon$  in SRII phase, see [47]. In this picture,  $h$  measures the sharpness of the transition of the mode function towards its final attractor value in SRII phase. For a sharp transition, we require  $|h| \gg 1$ . To simplify the analysis, as in [1], here we take  $h = -6$  so  $\epsilon_V = \epsilon_e$ . Finally, note that there is the term  $\eta'$  in  $\mathbf{H}_4$  which induces a delta-function type contribution in Hamiltonian. This is because,  $\eta$  un-

dergoes a sudden jump at the onset of transition from the USR phase to the SRII phase.

To calculate the loop corrections via in-in formalism, we need the mode function of  $\mathcal{R}$  in all three phases. Starting with the Bunch-Davies (Minkowski) initial condition, the mode function in the first SR phase is given by

$$\mathcal{R}_k^{(1)} = \frac{H}{M_P \sqrt{4\epsilon_i k^3}} (1 + ik\tau) e^{-ik\tau}. \quad (3)$$

Assuming an instant transition to USR phase at  $\tau = \tau_i$ , and imposing the matching condition for the continuity of  $\mathcal{R}$  and its derivative, the mode function in the USR phase is obtained to be,

$$\mathcal{R}_k^{(2)} = \frac{H}{M_P \sqrt{4\epsilon_i k^3}} \left( \frac{\tau_i}{\tau} \right)^3 \left[ \alpha_k^{(2)} (1 + ik\tau) e^{-ik\tau} + \beta_k^{(2)} c.c. \right], \quad (4)$$

where c.c. stands for complex conjugate, [51]. By doing matching conditions,  $\alpha_k^{(2)}$  and  $\beta_k^{(2)}$  read

$$\alpha_k^{(2)} = 1 + \frac{3i}{2k^3 \tau_i^3} (1 + k^2 \tau_i^2), \quad \beta_k^{(2)} = \frac{3i}{2k^3 \tau_i^3} (-1 + ik\tau_i)^2. \quad (5)$$

Finally, imposing the matching conditions at the end of USR phase,  $\tau_e$ , the outgoing mode function in the final attractor phase (SRII) is given by,

$$\mathcal{R}_k^{(3)} = \frac{H}{M_P \sqrt{4\epsilon(\tau) k^3}} \left[ \alpha_k^{(3)} (1 + ik\tau) e^{-ik\tau} + \beta_k^{(3)} c.c. \right], \quad (6)$$

in which the coefficients  $\alpha_k^{(3)}$  and  $\beta_k^{(3)}$  are given in equations A4 and A5 in the appendix A.

Before we proceed, it is helpful to address several key points carefully: a) with the UV-IR cutoff regularization approach, we use the IR and UV nondynamic cutoffs to regularize adequately the two point function divergences b) for the computation of time integrals, we perform the time regularization by utilizing the  $i\varepsilon$  prescription and the principle value technique, c) to perform the calculations we utilize the well-established perturbative in-in formalism.

According to in-in formalism, the expectation value of a typical operator, to second order in perturbation theory, is expressed as

$$\begin{aligned} \langle \mathcal{O}(\tau) \rangle_\Omega &\simeq \langle \mathcal{O}_I(\tau) \rangle_0 + 2\text{Im} \int_{-\infty}^{\tau} d\tau' \langle \mathcal{O}_I(\tau) H_I(\tau') \rangle_0 \\ &+ \int_{\tau_0}^{\tau} d\tau_1 \int_{\tau_0}^{\tau} d\tau_2 \langle H_I(\tau_1) \mathcal{O}_I(\tau) H_I(\tau_2) \rangle_0 \\ &- 2\text{Re} \int_{\tau_0}^{\tau} d\tau_1 \int_{\tau_0}^{\tau_1} d\tau_2 \langle \mathcal{O}_I(\tau) H_I(\tau_1) H_I(\tau_2) \rangle_0. \end{aligned} \quad (7)$$

We use  $\langle \Omega | \mathcal{O}(\tau) | \Omega \rangle \equiv \langle \mathcal{O}(\tau) \rangle_\Omega$  and  $\langle 0 | \mathcal{O}(\tau) | 0 \rangle \equiv \langle \mathcal{O}(\tau) \rangle_0$ , where subscripts  $\Omega$  and 0 refer the interacting and free vacuums respectively,

We now proceed to calculate the contributions arising from loop corrections, starting with a detailed analysis of the quartic diagram. Then we calculate the contributions associated to the cubic diagram which is much complicated due to the nested integrals, as shown in figure 1. Our analysis shows that the tadpole contributions are also as important as the two other contributions. To evaluate the tadpole terms, we employ the Mukhanov-Sasaki (M-S) equation for the zero-mode solution. By imposing constraints from the CMB and also considering the transitions SRI  $\rightarrow$  USR and USR  $\rightarrow$  SRI, we find the solutions for tadpole contribution, see appendix C.

*Contributions from Quartic Hamiltonian.*-The one-loop correction in power spectrum induced from quartic Hamiltonian for the USR phase is expressed as follows

$$2M_P^2 \delta_{k_1 k_2} \int_{-\infty}^0 d\tau' \int_0^\infty \frac{d^3 \mathbf{q}}{(2\pi)^3} (I_1 + 4I_2 + I_3)(\tau'), \quad (8)$$

where  $\delta_{k_1 k_2} \equiv (2\pi)^3 \delta^3(\mathbf{k}_1 + \mathbf{k}_2)$  and  $I_i$  expressions are defined in A1-A3 in appendix A. In our convention,  $\mathbf{k}$  represents the long CMB mode while  $\mathbf{q}$  represent the mode which runs inside the loop.

Combining the relevant results for A1-A3, and by employing cutoff renormalization techniques, for each part

of the bulk of USR phase, i.e.  $\tau_i < \tau < \tau_e$ , we obtain

$$\langle \mathcal{R}_{k_1}^{(2)}(\tau_0) \mathcal{R}_{k_2}^{(2)}(\tau_0) \rangle_{\Omega_{I1bu}} = -\frac{36H^4}{64\pi^2 M_P^4 \epsilon_i^2 k^3} e^{6\Delta\mathcal{N}} \delta_{k_1 k_2} \times \left[ (3 \log(-M \tau_i) + 3\gamma_{EM} - 2 + 3 \log(2)) \right], \quad (9)$$

$$\langle \mathcal{R}_{k_1}^{(2)}(\tau_0) \mathcal{R}_{k_2}^{(2)}(\tau_0) \rangle_{\Omega_{I2bu}} = \frac{24H^4}{64\pi^2 M_P^4 \epsilon_i^2 k^3} e^{6\Delta\mathcal{N}} \delta_{k_1 k_2} \quad (10)$$

$$\times \left[ (3 \log(-M \tau_i) + 3\gamma_{EM} - 2 + 3 \log(2)) \right],$$

and

$$\langle \mathcal{R}_{k_1}^{(2)}(\tau_0) \mathcal{R}_{k_2}^{(2)}(\tau_0) \rangle_{\Omega_{I3bu-grad}} = \frac{-189H^4}{128\pi^2 M_P^4 \epsilon_i^2 k^3} e^{4\Delta\mathcal{N}} \times \delta_{k_1 k_2} \left[ (2 \log(-M \tau_i) + 2\gamma_{EM} - 3 + 2 \log(2)) \right]. \quad (11)$$

Note the logarithmic term which is the hallmark of the quantum loop corrections.

It is evident that the leading terms are of the order  $e^{6\Delta\mathcal{N}}$ , while the third term, which originates from the gradient interactions, is of the order  $e^{4\Delta\mathcal{N}}$  and is therefore negligible in comparison. Here,  $\gamma_{EM}$  represents the Euler-Mascheroni constant. The integrands, however, exhibit divergences, and according to Fubini's theorem, it is not permissible to interchange the order of integration and, integration with series, in such cases. Moreover, careful attention must be given to the order of momentum and time integrations, as improper handling of these steps can lead to inconsistencies. These challenges motivated us to adopt the cutoff regularization technique as a systematic approach to handle these divergences. In this method, we impose finite integration bounds, specifically  $\int_m^M$ , where  $m \rightarrow 0$  and  $M \rightarrow \infty$ . After performing the momentum integration, the series expansion is carried out in two distinct regimes: first, in the UV limit, by expanding around  $M \rightarrow \infty$  to examine the high-energy behavior; and second, in the IR limit, by expanding around  $m \rightarrow 0$  to explore the low-energy contributions. This dual expansion allows us to systematically study both UV and IR divergences and their respective contributions to the overall result.

From an order-of-magnitude perspective, this result for the USR phase is consistent with previously reported results in the literature [1, 3].

Now, by following a similar procedure, we can calculate the contributions of the localized source term  $\delta(\tau - \tau_e)$  encoded in  $\eta'$  at the end of USR, yielding

$$\langle \mathcal{R}_{k_1}^{(2)}(\tau_0) \mathcal{R}_{k_2}^{(2)}(\tau_0) \rangle_{\Omega_{I1tr}} = \frac{12H^4}{64\pi^2 M_P^4 \epsilon_i^2 k^3} e^{6\Delta\mathcal{N}} \delta_{k_1 k_2} \times \left[ (3 \log(-M \tau_i) + 3\gamma_{EM} - 2 + 3 \log(2)) \right], \quad (12)$$

$$\langle \mathcal{R}_{k_1}^{(2)}(\tau_0) \mathcal{R}_{k_2}^{(2)}(\tau_0) \rangle_{\Omega_{I2tr}} = \frac{-24H^4}{64\pi^2 M_P^4 \epsilon_i^2 k^3} e^{6\Delta\mathcal{N}} \delta_{k_1 k_2} \times \left[ (3 \log(-M \tau_i) + 3\gamma_{EM} - 2 + 3 \log(2)) \right], \quad (13)$$

while for the gradient term we obtain

$$\langle \mathcal{R}_{k_1}^{(2)}(\tau_0) \mathcal{R}_{k_2}^{(2)}(\tau_0) \rangle_{\Omega_{I3tr-rad}} = \frac{-9H^4}{64\pi^2 M_P^4 \epsilon_i^2 k^3} e^{4\Delta\mathcal{N}} \times \delta_{k_1 k_2} \left[ (2 \log(-M \tau_1) + 2\gamma_{EM} - 3 + 2 \log(2)) \right]. \quad (14)$$

It should be noted that, as in [1], here we consider the case  $h = -6$  so the contributions from SR II phase is negligible. In a separate work we will consider a general value of  $h$  and will examine the contributions in one-loop power spectrum from the SR II phase as well.

*Contributions from Cubic Hamiltonian.*—For the cubic action given in equation 1, and with the assistance of equation 7, the two-point correlation function for the USR phase can be expressed as

$$\begin{aligned} \langle \mathcal{R}_{k_1}^{(2)}(\tau_0) \mathcal{R}_{k_2}^{(2)}(\tau_0) \rangle_{\Omega_{H_3}} &\equiv \langle \mathcal{R}_{k_1 k_2}^{(2)}(\tau_0) \rangle_{\Omega_{H_3}} \\ &= - \int_{-\infty}^{\tau_0} d\tau_1 \int_{-\infty}^{\tau_1} d\tau_2 \left[ \int_0^{\infty} \frac{d^3 \mathbf{q}}{(2\pi)^3} \left[ \langle 0 | \mathbf{H}_3(\tau_1) \mathbf{H}_3(\tau_2) \mathcal{R}_{k_1 k_2}^{(2)}(\tau_0) | 0 \rangle \right. \right. \\ &\quad \left. \left. + \langle 0 | \mathcal{R}_{k_1 k_2}^{(2)}(\tau_0) \mathbf{H}_3(\tau_1) \mathbf{H}_3(\tau_2) | 0 \rangle \right] \right] \\ &\quad + \int_{-\infty}^{\tau_0} d\tau_1 \int_{-\infty}^{\tau_0} d\tau_2 \left( \int_0^{\infty} \frac{d^3 \mathbf{q}}{(2\pi)^3} \langle 0 | \mathbf{H}_3(\tau_1) \mathcal{R}_{k_1 k_2}^{(2)}(\tau_0) \mathbf{H}_3(\tau_2) | 0 \rangle \right). \end{aligned} \quad (15)$$

We need to address the complexity of the nested integrals in lines 3 and 4 of the above equation. During the USR phase, we encounter time divergences at both the upper and lower bounds of these integrals. To handle these divergences, we employ the well-established Cauchy principal value technique. This approach allows us to introduce a parameter that controls the rate at which the two integration boundaries approach each other, effectively detouring the infinities.

Using  $\mathbf{H}_3$  given in equation 1 into equation 15, the one-loop correction from  $\mathbf{H}_3$  has the following form,

$$\begin{aligned} \langle | \mathcal{R}_{k_1}^{(2)}(\tau_0) \mathcal{R}_{k_2}^{(2)}(\tau_0) | \rangle_{\Omega_{H_3}} &= \\ -8M_P^4 \int_{\tau_i}^{\tau_e} d\tau_1 \int_{\tau_i}^{\tau_1} d\tau_2 \int_0^{\infty} \frac{d^3 \mathbf{q}}{(2\pi)^3} \mathcal{G}(\tau_1, \tau_2; q), \end{aligned} \quad (16)$$

in which,  $\mathcal{G}(\tau_1, \tau_2; q)$  is defined in Equations B1 - B3 in Appendix B. To obtain the results, as we mentioned, it is crucial to handle the complexity of the nested integrals carefully. The integration is performed over the full time interval, specifically  $\tau_i \leq \tau_2 \leq \tau_1 \leq \tau_e$ . After renormalizing both UV and IR divergences, the one-loop correction in power spectrum of bulk term induced by  $\mathbf{H}_3$  takes the following form,

$$\langle \mathcal{R}_{k_1}^{(2)}(\tau_0) \mathcal{R}_{k_2}^{(2)}(\tau_0) \rangle_{\Omega_{H_3 bu}} = \frac{24H^4 e^{6\Delta\mathcal{N}}}{64M_P^4 \pi^2 \epsilon_i^2 k^3} \delta_{k_1 k_2}. \quad (17)$$

For the gradient terms B2 and B3, the results behave the same as (17), yielding

$$\langle \mathcal{R}_{k_1}^{(2)}(\tau_0) \mathcal{R}_{k_2}^{(2)}(\tau_0) \rangle_{\Omega_{H_3 gr}} = \frac{15H^4 e^{6\Delta\mathcal{N}}}{64M_P^4 \pi^2 \epsilon_i^2 k^3} \delta_{k_1 k_2}, \quad (18)$$

and

$$\langle \mathcal{R}_{k_1}^{(2)}(\tau_0) \mathcal{R}_{k_2}^{(2)}(\tau_0) \rangle_{\Omega_{H_3 sr}} = \frac{105H^4 e^{6\Delta\mathcal{N}}}{64M_P^4 \pi^2 \epsilon_i^2 k^3} \delta_{k_1 k_2}. \quad (19)$$

In the above analysis we have calculated the one-loop corrections from both quartic and cubic diagrams, taking into account the regularization. Combining all results so far, the leading regularized fractional one-loop correction in power spectrum,  $\frac{\Delta\mathcal{P}}{\mathcal{P}_{\text{CMB}}}$ , reads as,

$$\frac{\Delta\mathcal{P}}{\mathcal{P}_{\text{CMB}}} \simeq 33 \frac{\pi^2}{2} \mathcal{P}_{\text{CMB}} e^{6\Delta\mathcal{N}} (1 + c \ln(M\tau_i)), \quad (20)$$

in which  $\mathcal{P}_{\text{CMB}} = H^2/8\pi^2 M_P^2 \epsilon_i$  is the CMB scale power spectrum and  $c$  is a numerical factor. We see that our regularized one-loop correction has the same structure as advocated in [1, 3, 4].

*Contributions from Tadpole.*—We now focus on the contribution of the tadpole diagram, that is the zero-mode contribution. To evaluate the tadpole terms, we utilize the M-S equation for the zero-mode solution. By imposing constraints from the CMB superhorizon modes at the end of inflation on one hand and analyzing the transitions from *SRI* – *USR* and *USR* – *SR II* on the other, we derive the solutions for the tadpole zero modes, as presented in equations C1–C3 in Appendix C.

The corrections from the tadpole is given by,

$$\begin{aligned} \langle \mathcal{R}_{k_1}^{(2)}(\tau_0) \mathcal{R}_{k_2}^{(2)}(\tau_0) \rangle_{\Omega_{tad}} &= \\ -8M_P^4 \int_{\tau_i}^{\tau_e} d\tau_1 \int_{\tau_i}^{\tau_1} d\tau_2 \int_0^{\infty} \frac{d^3 \mathbf{q}}{(2\pi)^3} \mathcal{S}(\tau_1, \tau_2; q), \end{aligned} \quad (21)$$

where  $\mathcal{S}(\tau_1, \tau_2; q)$  appears in C4. For the bulk of the tadpole contribution we obtain,

$$\begin{aligned} \langle \mathcal{R}_{k_1}^{(2)}(\tau_0) \mathcal{R}_{k_2}^{(2)}(\tau_0) \rangle_{\Omega_{tad-bu}} &= \\ \frac{72H^4 e^{6\Delta\mathcal{N}}}{64M_P^4 \pi^2 \epsilon_i^2 k^3} \delta_{k_1 k_2} (\cos(1) - \sin(1)) \\ \left[ (3 \log(-M \tau_1) + 3\gamma_{EM} - 2 + 3 \log(2)) \right], \end{aligned} \quad (22)$$

while for the gradient term the result is subleading, obtaining

$$\begin{aligned} \langle \mathcal{R}_{k_1}^{(2)}(\tau_0) \mathcal{R}_{k_2}^{(2)}(\tau_0) \rangle_{\Omega_{tad-gr}} &= \\ \frac{243H^4 e^{4\Delta\mathcal{N}}}{256M_P^4 \pi^2 \epsilon_i^2 k^3} \delta_{k_1 k_2} (\cos(1) - \sin(1)) \\ \left[ (2 \log(-M \tau_1) + 2\gamma_{EM} - 3 + 2 \log(2)) \right]. \end{aligned} \quad (23)$$

The results of 22 can be expressed as follows

$$\frac{\Delta\mathcal{P}}{\mathcal{P}_{\text{CMB}}} = 72\pi^2 (\cos(1) - \sin(1)) \mathcal{P}_{\text{CMB}} e^{6\Delta\mathcal{N}} \times \left[ (3 \log(-M \tau_i) + 3\gamma_{EM} - 2 + 3 \log(2)) \right]. \quad (24)$$

We see that this also has the same form as in Eq. (20).

*Conclusion.*—In the ongoing debates concerning the one-loop correction in models of USR inflation, there are three different claims. The first category claims that the fractional loop corrections scale like the peak of power spectrum at the end of USR as in (20), the second category claims that the loop corrections are suppressed by the slow-roll parameter  $\epsilon$ , while the third category claims that the loop corrections are nearly zero (volume suppressed).

To address the one-loop corrections within QFT, there are a number of important points to keep in mind. First, any QFT corrections must be addressed using rigorous regularization and renormalization techniques. To tackle the momentum divergences, we used the cutoff regularization method. Second, the calculations must account for the full range of momenta and time intervals, meaning all contributing modes from zero to infinity must be considered. For time divergences, especially in nested integrals, we relied on the Cauchy P.V. technique, besides the conventional  $i\epsilon$  prescription. Although these calculations are intricate, we ensured that these critical steps were included in our analysis. It turns out that handling the momentum and time integrals are non-trivial. Careful attentions must be paid to the order of integrations, series expansions, and limits. With these considerations in mind, and despite the tedious and time-consuming nature of the process, we have presented concrete results for the regularized one-loop corrections.

We have considered all one-loop diagrams, including the tadpole contribution. Our analysis shows that the renormalized one-loop corrections scale like  $\mathcal{P}_{\text{CMB}} e^{6\Delta\mathcal{N}}$  so it can get out of perturbative control if the duration of the USR phase is long enough. Our result is in agreement with the results of the first category listed above, such as in [1, 3, 4]. However, to simplify the analysis, as in [1], we have considered the setup with a sharp transition in which the mode function quickly approaches its final attractor value. However, one may consider a mild transition in which the mode functions keep evolving during SRII phase. This brings additional complexities and the one-loop correction can receive slow-roll suppression as claimed by second category such as in [5, 6, 20, 26].

Moving forward, it might be worthwhile to revisit this problem using other methods like stochastic approach while it is natural to go beyond, say calculations of renormalized two-loop corrections [48, 49], to see the behaviour of these corrections. We plan to address these questions in future works.

*Acknowledgment.*— We are grateful to Hassan Firouzjahi for critically reviewing the initial draft of the paper

and providing constructive suggestions. We also thank Sina Hooshangi for valuable discussions.

## Appendix A: Quartic Hamiltonian Integrands and Coefficients

Integrands belonging to USR phase:

$$I_1 = \tilde{I} |\mathcal{R}'_{\mathbf{q}}(\tau)|^2 \text{Im} \left[ \mathcal{R}_{\mathbf{k}}^*(\tau_0)^2 \mathcal{R}_{\mathbf{k}}(\tau)^2 \right], \quad (A1)$$

$$I_2 = \tilde{I} \text{Im} \left[ \mathcal{R}_{\mathbf{k}}^*(\tau_0)^2 \phi_{\mathbf{k}}(\tau) \mathcal{R}'_{\mathbf{k}}(\tau) \mathcal{R}_{\mathbf{q}}(\tau) \mathcal{R}'_{\mathbf{q}}(\tau)^* \right], \quad (A2)$$

$$I_3 = \bar{I} q^2 |\mathcal{R}_{\mathbf{q}}(\tau)|^2 \text{Im} \left[ \mathcal{R}_{\mathbf{k}}^*(\tau_0)^2 \mathcal{R}_{\mathbf{k}}(\tau)^2 \right]. \quad (A3)$$

where  $\tilde{I} \equiv \left( \eta^2 - \frac{\eta'}{aH} \right) a^2(\tau)$  and  $\bar{I} \equiv \left( \eta^2 + \frac{\eta'}{aH} \right) a^2(\tau)$ . The coefficients appeared in (6) obtained from the matching conditions:

$$\alpha_k = \frac{1}{8k^6 \tau_i^3 \tau_e^3} \left[ 3h(1 - ik\tau_e)^2 (1 + ik\tau_i)^2 e^{2ik(\tau_e - \tau_i)} - i(2k^3 \tau_i^3 + 3ik^2 \tau_i^2 + 3i)(4ik^3 \tau_e^3 - hk^2 \tau_e^2 - h) \right], \quad (A4)$$

$$\beta_k = \frac{-1}{8k^6 \tau_i^3 \tau_e^3} \left[ 3(1 + ik\tau_i)^2 (h + hk^2 \tau_e^2 + 4ik^3 \tau_e^3) e^{-2ik\tau_i} + ih(1 + ik\tau_e)^2 (3i + 3ik^2 \tau_i^2 + 2k^3 \tau_i^3) e^{-2ik\tau_e} \right]. \quad (A5)$$

Definitely the coefficients  $\alpha_k^*$  and  $\beta_k^*$  can be obtained in same procedure.

## Appendix B: Cubic Hamiltonian Integrands and Coefficients

Here the definition of  $\mathcal{G}(\tau_1, \tau_2; k)$  and its components are introduced:

$$\mathcal{G}(\tau_1, \tau_2; q) \equiv \text{Im} \left[ G^*(\tau_2) g_k^*(\tau_2) (Z(\tau_1) + 2Y(\tau_1)) \right] \quad (B1)$$

$$+ \text{Im} \left[ G^*(\tau_2) [(Z(\tau_1) + 2Y(\tau_1)) - g_k(\tau_1) Z(\tau_1)] \right] \quad (B2)$$

$$+ \text{Im} \left[ \tilde{G}^*(\tau_2) \tilde{Z}(\tau_1) \right] \quad (B3)$$

where

$$\begin{aligned} G^*(\tau_2) &= \eta \epsilon a^2 \mathcal{R}_{\mathbf{k}}^*(\tau_0) \mathcal{R}_{\mathbf{k}}(\tau_2) \mathcal{R}'_{\mathbf{q}}(\tau_2)^2, \\ \tilde{G}^*(\tau_2) &= \mathbf{q}^2 \eta \epsilon a^2 \mathcal{R}_{\mathbf{k}}^*(\tau_0) \mathcal{R}_{\mathbf{k}}(\tau_2) \mathcal{R}_{\mathbf{q}}(\tau_2)^2, \\ Z(\tau_1) &= 2\epsilon \eta a^2 \mathcal{R}'_{\mathbf{q}}(\tau_1)^2 \text{Im} \left[ \Phi_{\mathbf{k}}^*(\tau_0) \mathcal{R}_{\mathbf{k}}(\tau_1) \right], \\ \tilde{Z}(\tau_1) &= 2\mathbf{q}^2 \epsilon \eta a^2 \mathcal{R}_{\mathbf{q}}(\tau_1)^2 \text{Im} \left[ \mathcal{R}_{\mathbf{k}}^*(\tau_0) \mathcal{R}_{\mathbf{k}}(\tau_1) \right], \\ Y(\tau_1) &= 2\epsilon \eta a^2 \mathcal{R}'_{\mathbf{q}}(\tau_1) \mathcal{R}_{\mathbf{q}}(\tau_1) \text{Im} \left[ \mathcal{R}_{\mathbf{k}}^*(\tau_0) \mathcal{R}'_{\mathbf{k}}(\tau_1) \right], \end{aligned} \quad (B4)$$

$$g_{\mathbf{q}}(\tau) = \frac{(\partial \mathcal{R}_{\mathbf{q}})^2}{\mathcal{R}_{\mathbf{q}}'^2} = \frac{q^2 \mathcal{R}_{\mathbf{q}}^2}{\mathcal{R}_{\mathbf{q}}'^2}.$$

### Appendix C: Tadpole Calculations

Here we briefly discuss the results for tadpole contribution, from figure 1. Whereas the vertices are of order 3 we employ  $\mathbf{H}_3$  Hamiltonian for the calculations. Accordingly we need to calculate zero modes for each phases of our multi phase USR prototype. By solving the M-S equation for  $k = 0$  for the SRI it can be obtained as

$$\mathcal{Q}_{k=0}^{(1)} = c_1 \tau^3 + c_2, \quad (\text{C1})$$

then for USR period one has

$$\mathcal{Q}_{k=0}^{(2)} = d_1 \frac{1}{\tau^3} + d_2. \quad (\text{C2})$$

After matching conditions for the coefficients we obtain

$$d_1 = H/\sqrt{\bar{k}^3 \epsilon_i},$$

$$d_2 = (3 - 3i)(-(1 + i) + e^i) H \bar{k}^{3/2} t_i^6 / 2\sqrt{\epsilon_i},$$

where  $\bar{k}$  stands for superhorizon mode. Following a same procedure the mode function of SRII reads

$$\mathcal{Q}_{k=0}^{(3)} = e_1 \tau^3 + e_2. \quad (\text{C3})$$

To do the matching conditions, in order to get the constants of above equations, we need to impose the constraints from beginning of inflation, end of inflation and transitions. By utilizing the cubic Hamiltonians the contribution of tadpole diagram can be expressed as follows

$$\mathcal{S}(\tau_1, \tau_2; q) \equiv -4\text{Im} \left[ [\Delta(\tau_1)] \times (X(\tau_2) + W(\tau_2)) \right]. \quad (\text{C4})$$

$$\Delta(\tau_1) = 2\eta\epsilon a^2 \left[ \text{Im} [\mathcal{R}_k^*(\tau_0)^2 \mathcal{R}_q(\tau_1) \mathcal{R}'_q(\tau_1)] \mathcal{Q}'_0(\tau_1) \right],$$

$$X(\tau_2) = 2\eta\epsilon a^2 \left[ \mathcal{Q}_0(\tau_2) |\mathcal{R}'_q(\tau_2)|^2 \right], \quad (\text{C5})$$

$$W(\tau_2) = 2\mathbf{q}^2 \eta\epsilon a^2 \left[ \mathcal{Q}_0(\tau_2) |\mathcal{R}_q(\tau_2)|^2 \right].$$

- 
- [1] J. Kristiano and J. Yokoyama, Phys. Rev. Lett. **132**, no.22, 221003 (2024) [arXiv:2211.03395 [hep-th]].
- [2] J. Kristiano and J. Yokoyama, Phys. Rev. D **109**, no.10, 103541 (2024), [arXiv:2303.00341 [hep-th]].
- [3] H. Firouzjahi, JCAP **10**, 006 (2023)
- [4] H. Firouzjahi, Phys. Rev. D **109**, no.4, 043514 (2024).
- [5] A. Riotto, [arXiv:2301.00599 [astro-ph.CO]].
- [6] A. Riotto, [arXiv:2303.01727 [astro-ph.CO]].
- [7] S. Maity, H. V. Ragavendra, S. K. Sethi and L. Sriramkumar, JCAP **05**, 046 (2024)
- [8] S. Choudhury, S. Panda and M. Sami, Phys. Lett. B **845**, 138123 (2023), [arXiv:2302.05655 [astro-ph.CO]].
- [9] S. Choudhury, S. Panda and M. Sami, JCAP **11**, 066 (2023), [arXiv:2303.06066 [astro-ph.CO]].
- [10] S. Choudhury, S. Panda and M. Sami, JCAP **08**, 078 (2023), [arXiv:2304.04065 [astro-ph.CO]].
- [11] P. Ivanov, P. Naselsky and I. Novikov, Phys. Rev. D **50**, 7173-7178 (1994).
- [12] J. Garcia-Bellido and E. Ruiz Morales, Phys. Dark Univ. **18**, 47-54 (2017).
- [13] C. Germani and T. Prokopec, Phys. Dark Univ. **18**, 6-10 (2017).
- [14] M. Biagetti, G. Franciolini, A. Kehagias and A. Riotto, JCAP **07**, 032 (2018).
- [15] M. Y. Khlopov, Res. Astron. Astrophys. **10**, 495-528 (2010), [arXiv:0801.0116 [astro-ph]].
- [16] O. Özsoy and G. Tasinato, Universe **9**, no.5, 203 (2023), [arXiv:2301.03600 [astro-ph.CO]].
- [17] C. T. Byrnes and P. S. Cole, [arXiv:2112.05716 [astro-ph.CO]].
- [18] A. Escrivà, F. Kuhnel and Y. Tada, [arXiv:2211.05767 [astro-ph.CO]].
- [19] S. Hooshangi, A. Talebian, M. H. Namjoo and H. Firouzjahi, Phys. Rev. D **105**, no.8, 083525 (2022) [arXiv:2201.07258 [astro-ph.CO]].
- [20] H. Firouzjahi and A. Riotto, JCAP **02**, 021 (2024) [arXiv:2304.07801 [astro-ph.CO]].
- [21] J. Kristiano and J. Yokoyama, [arXiv:2405.12149 [astro-ph.CO]].
- [22] S. Raatikainen, S. Räsänen and E. Tomberg, Phys. Rev. Lett. **133**, no.12, 121403 (2024) [arXiv:2312.12911 [astro-ph.CO]].
- [23] S. Pi, [arXiv:2404.06151 [astro-ph.CO]].
- [24] S. L. Cheng, D. S. Lee and K. W. Ng, JCAP **03**, 008 (2024) [arXiv:2305.16810 [astro-ph.CO]].
- [25] K. Inomata, M. Braglia, X. Chen and S. Renaux-Petel, JCAP **04**, 011 (2023) [erratum: JCAP **09**, E01 (2023)] [arXiv:2211.02586 [astro-ph.CO]].
- [26] L. Iacconi, D. Mulryne and D. Seery, JCAP **06**, 062 (2024) [arXiv:2312.12424 [astro-ph.CO]].
- [27] K. Inomata, Phys. Rev. Lett. **133**, no.14, 141001 (2024) [arXiv:2403.04682 [astro-ph.CO]].
- [28] J. Fumagalli, [arXiv:2305.19263 [astro-ph.CO]].
- [29] J. Fumagalli, [arXiv:2408.08296 [astro-ph.CO]].
- [30] Y. Tada, T. Terada and J. Tokuda, JHEP **01**, 105 (2024)
- [31] R. Kawaguchi, S. Tsujikawa and Y. Yamada, [arXiv:2407.19742 [hep-th]].
- [32] K. Inomata and X. Luo, [arXiv:2410.07086 [astro-ph.CO]].
- [33] A. Caravano, K. Inomata and S. Renaux-Petel, Phys. Rev. Lett. **133**, no.15, 15 (2024) [arXiv:2403.12811 [astro-ph.CO]].
- [34] B. S. DeWitt, Phys. Rept. **19**, 295-357 (1975).
- [35] N. D. Birrell and P. C. W. Davies, Cambridge Univ.

- Press, 1984.
- [36] S. A. Fulling, London Math. Soc. Student Texts **17**, 1-315 (1989)
- [37] L. E. Parker and D. Toms, Cambridge University Press, 2009.
- [38] S. Weinberg, Phys. Rev. D **72**, 043514 (2005) [arXiv:hep-th/0506236 [hep-th]].
- [39] X. Chen, Y. Wang and Z. Z. Xianyu, JHEP **08**, 051 (2016) [arXiv:1604.07841 [hep-th]].
- [40] H. Sheikahmadi, Eur. Phys. J. C **79**, no.6, 451 (2019) [arXiv:1901.01905 [gr-qc]].
- [41] C. Animali, P. Conzini and G. Marozzi, JCAP **05**, no.05, 026 (2022) [arXiv:2201.05602 [gr-qc]].
- [42] G. Ballesteros and J. G. Egea, JCAP **07**, 052 (2024) [arXiv:2404.07196 [astro-ph.CO]].
- [43] L. Senatore and M. Zaldarriaga, JHEP **12**, 008 (2010) [arXiv:0912.2734 [hep-th]].
- [44] C. Cheung, P. Creminelli, A. L. Fitzpatrick, J. Kaplan and L. Senatore, JHEP **0803**, 014 (2008).
- [45] C. Cheung, A. L. Fitzpatrick, J. Kaplan and L. Senatore, JCAP **0802**, 021 (2008).
- [46] H. Firouzjahi, [arXiv:2403.03841 [astro-ph.CO]].
- [47] Y. F. Cai, X. Chen, M. H. Namjoo, M. Sasaki, D. G. Wang and Z. Wang, JCAP **05**, 012 (2018) [arXiv:1712.09998 [astro-ph.CO]].
- [48] Work in progress.
- [49] Work in progress.
- [50] *For example, some earlier studies evaluated integrals over restricted momentum ranges, such as from  $k$  to  $k^*$ , rather than the full range from 0 to  $\infty$ . This selective treatment can significantly impact loop corrections by excluding contributions from certain modes.*
- [51] *Our calculations have been done in both Mathematica 13.2 and Maple 2019 and showed no difference.*